



**HAL**  
open science

## Probing the circuits of conscious perception with magnetophosphenes

Julien Modolo, Mahmoud Hassan, Giulio Ruffini, Alexandre Legros

► **To cite this version:**

Julien Modolo, Mahmoud Hassan, Giulio Ruffini, Alexandre Legros. Probing the circuits of conscious perception with magnetophosphenes. *Journal of Neural Engineering*, 2020, 17 (3), pp.036034. 10.1088/1741-2552/ab97f7 . hal-02798352

**HAL Id: hal-02798352**

**<https://univ-rennes.hal.science/hal-02798352>**

Submitted on 23 Jun 2020

**HAL** is a multi-disciplinary open access archive for the deposit and dissemination of scientific research documents, whether they are published or not. The documents may come from teaching and research institutions in France or abroad, or from public or private research centers.

L'archive ouverte pluridisciplinaire **HAL**, est destinée au dépôt et à la diffusion de documents scientifiques de niveau recherche, publiés ou non, émanant des établissements d'enseignement et de recherche français ou étrangers, des laboratoires publics ou privés.

## Probing the circuits of conscious perception with magnetophosphenes

Julien Modolo<sup>1,2,\* †</sup>, Mahmoud Hassan<sup>1,3 †</sup>, Giulio Ruffini<sup>4</sup>, Alexandre Legros<sup>2,5,6,7</sup>

<sup>1</sup>Univ Rennes, INSERM, LTSI – U1099, F-35000 Rennes, France.

<sup>2</sup>Human Threshold Research Group, Lawson Health Research Institute, London (ON), Canada.

<sup>3</sup>NeuroKyma, F-35000 Rennes, France

<sup>4</sup>Starlab Barcelona, Barcelona, Spain.

<sup>5</sup>Departments of Medical Biophysics and Medical Imaging, Western University, London, ON, Canada

<sup>6</sup>School of Kinesiology, Western University, London, ON, Canada

<sup>7</sup>EuroMov, Université de Montpellier, France

\*Correspondance: Julien Modolo – [julien.modolo@inserm.fr](mailto:julien.modolo@inserm.fr) - Laboratoire Traitement du

Signal et de l'Image (LTSI), Bâtiment 22 Campus de Beaulieu, 35042 Rennes Cedex, France

†Co-first authors (equally contributed).

## Abstract

**Background:** We aimed at characterizing, in non-invasive human brain recordings, the large-scale, coordinated activation of distant brain regions thought to occur during conscious perception. This process is termed ignition in the Global Workspace Theory, and integration in Integrated Information Theory, which are two of the major theories of consciousness.

**Approach:** Here, we provide evidence for this process in humans by combining a magnetically-induced phosphene perception task with electroencephalography. Functional cortical networks were identified and characterized using graph theory to quantify the impact of conscious perception on local (segregation) and distant (integration) processing.

**Main results:** Conscious phosphene perception activated frequency-specific networks, each associated with a specific spatial scale of information processing. Integration increased within an alpha-band functional network, while segregation occurred in the beta band.

**Significance:** These results bring novel evidence for the functional role of distinct brain oscillations and confirm the key role of integration processes for conscious perception in humans.

**Keywords:** electroencephalography, conscious perception, functional connectivity, brain stimulation

## Introduction

The characterization of the physiological mechanisms that enable conscious perception is the focus of intense, multi-disciplinary research efforts. As opposed to the question of the nature of consciousness itself (referred to as the “hard problem” of consciousness (Harnad, 1998)), the identification and characterization of the physiological processes that enable the emergence and maintenance of consciousness (referred to as the “easy problem” of consciousness (Harnad, 1998)) is more readily achievable. Two theories of consciousness are currently dominant in the field, namely the Global Workspace Theory (GWT (Dehaene et al., 1998; Dehaene et al., 2006; Dehaene and Changeux, 2011)), and the Integrated Information Theory (IIT (Tononi, 2004)). While both share some key common points, such as information processing being at the core of conscious processes and that information needs to be *integrated* at a large scale to be efficiently shared and processed, IIT also posits that conscious experience involves a sufficiently “complex” level of information processing. Another recent theory, the Kolmogorov theory (KT) of consciousness (Ruffini, 2017), also establishes links between the algorithmic complexity of information processed by cortical networks and conscious processes. The idea that information processing coordinated between distant brain regions is essential has received considerable experimental support, notably from combined transcranial magnetic stimulation-electroencephalography (TMS-EEG) studies in disorders of consciousness (DOC) patients and healthy controls: during unconsciousness (e.g., deep sleep, Propofol anesthesia or coma), TMS-evoked EEG responses fail to propagate in cortico-cortical networks and only induce local activation, while complex spatiotemporal responses are evoked at the brain-scale during wakefulness (Casali et al., 2013).

One of the processes proposed to enable the large-scale cortical activation associated with conscious processes is termed *ignition* in GWT, and consists of a sudden and coordinated large-scale recruitment of distant brain regions that can make information

1  
2  
3 available to the global workspace, enabling information processing (Dehaene and Changeux,  
4 2011). Ignition has been identified using functional MRI (fMRI) in a variety of tasks, as  
5 reviewed by Dehaene and Changeux (Dehaene and Changeux, 2011). A compelling example  
6 is that, during subliminal perception of words, the activated brain network is considerably less  
7 spatially extended than during conscious perception (Dehaene et al., 2001). Using EEG and  
8 magnetoencephalography (MEG), it has also been shown that a large-scale activation in the  
9 beta band within the fronto-parieto-temporal network is involved in the report of target  
10 stimuli (Gross et al., 2004). Invasive intracranial recordings have also been performed in  
11 humans using deep electrodes during exposure to masked/unmasked words, which revealed  
12 an increase in gamma power in distant sites in association with a beta synchrony increase. In a  
13 recent experimental study, van Vugt et al. provided compelling evidence for the ignition  
14 process in monkeys, using intracranial electrodes during a phosphene perception task (van  
15 Vugt et al., 2018). Phosphenes are visual perceptions in the absence of light, and can triggered  
16 by electric stimulation (electro-phosphenes (Lovsund et al., 1980a)) or magnetic stimulation  
17 (magneto-phosphenes (Lovsund et al., 1980b)). In this study, van Vugt et al. performed  
18 intracranial stimulation of the visual cortex in monkeys at different current intensities (sub-  
19 threshold vs. supra-threshold) and linked visual saccades with phosphene perception.  
20 Consistent with predictions from GWT or IIT, large-scale brain activation was observed at the  
21 onset of phosphene perception.  
22  
23  
24  
25  
26  
27  
28  
29  
30  
31  
32  
33  
34  
35  
36  
37  
38  
39  
40  
41  
42  
43  
44  
45  
46

47 In the present study, we aimed at inducing magnetophosphene percepts to characterize  
48 non-invasively the associated ignition process in humans. Our study involved twenty human  
49 subjects exposed to a 50 Hz magnetic field (MF) at 11 different flux density conditions given  
50 in a random order (5 mT steps ranging from 0 -sham- to 50 mT, each repeated 5 times for a  
51 total of 55 epochs per subject), while dense-EEG (64 channels) was recorded. Each epoch of  
52 exposure lasted 5 seconds, which was chosen to keep reasonable the duration of the  
53  
54  
55  
56  
57  
58  
59  
60

1  
2  
3 experiment. MF exposure was delivered through a whole-brain exposure system designed and  
4 manufactured in-house (Fig. 1A), which exposed the whole brain and eyeballs to a  
5 homogeneous level of MF. Large-scale functional connectivity was estimated from dense-  
6 EEG measurements using source connectivity analysis (Hassan and Wendling, 2018), and  
7 graph theory metrics were used to quantify local and global/distant processing, enabling the  
8 identification of nodes in a cortical network. The study design is summarized in Fig. 1. Our  
9 hypothesis was that, during suprathreshold (conscious) magnetophosphene perception, a  
10 drastic increase in global/distant processing characteristic of ignition occurs, which should be  
11 detectable through an increase in network integration quantified by graph theory based  
12 metrics.  
13  
14  
15  
16  
17  
18  
19  
20  
21  
22  
23  
24  
25  
26  
27  
28

## 29 **Materials and Methods**

### 30 *Experimental protocol*

31  
32  
33 This study was approved by the Health Sciences Research Ethics Board of Western  
34 University (London, ON, Canada) under the reference HSREB#18882. All experiments were  
35 performed in accordance with the relevant guidelines and regulations. Informed consent was  
36 obtained for the N=20 healthy volunteers who were recruited (age: 23.4 +/- 1.4, 10 males and  
37 10 females). Exclusion criteria ensure that study participants had no cardiovascular,  
38 neurological or visual system disorder. They were equipped with a 64 MRI-compatible EEG  
39 cap (Maglink, Compumedics-Neuroscan, US). Subjects were asked to sit in the chair placed  
40 below the MF exposure device and the coils were lowered so subjects had their head  
41 centered in the device for the duration of the experiment. EEG was continuously recorded,  
42 and subjects were asked to remain eyes closed for the duration of the experiment. An  
43 adaptation time to the darkness of the room of 5 minutes was present at the beginning of the  
44 exposure sequence. The 55 MF exposure conditions were then randomly delivered through a  
45  
46  
47  
48  
49  
50  
51  
52  
53  
54  
55  
56  
57  
58  
59  
60

1  
2  
3 custom-made LabView (National Instruments, USA) program, had a duration of 5 seconds  
4  
5 each, and were separated by 5 seconds. Each time that the participant began to perceive  
6  
7 magnetophosphenes, he/she had to press as fast as possible on a button directly synchronized  
8  
9 with the EEG acquisition system.  
10  
11  
12  
13

#### 14 *MF exposure device and physical principles*

15  
16  
17 The MF exposure device was used to deliver whole-brain exposure and consisted of  
18  
19 “Helmholtz-like” coils designed and manufactured in-house (for full details, please refer to  
20  
21 (Keenlside et al., 2013)). Let us mention that Helmholtz coils are a standard setup in physics  
22  
23 dating back to the end of the 19<sup>th</sup> century. The mean diameter of each coils was 50 cm and  
24  
25 their width 7.3 cm, and coils were separated by 20 cm. Water cooling (0.8 L/min) was used  
26  
27 through the squared hollow wire in order to prevent coil heating. MRI gradient amplifiers  
28  
29 (MTS corporation, USA) were used to power each coil (up to 200 A<sub>rms</sub> capability). The  
30  
31 experimental setup was Medical Grade approved by the Canadian Standard Association  
32  
33 (CSA). The MRI gradient amplifiers driving a 50 Hz current through the coils, which per  
34  
35 Maxwell-Ampere’s law generated a homogeneous 50 Hz MF at the level of the head and  
36  
37 eyes, which resulted in an induced electric field at the same frequency in these exposed  
38  
39 biological structures. Therefore, the MF exposure non-invasively generated induced fields and  
40  
41 current in the brain and retinal tissues at 50 Hz. Furthermore, let us note that the homogeneity  
42  
43 zone of the field included the entire brain (Keenlside et al., 2013).  
44  
45  
46  
47  
48  
49  
50

#### 51 *EEG acquisition and processing pipeline*

52  
53 64-channel EEG was acquired at a sampling frequency of 10 kHz and down-sampled  
54  
55 to 1 kHz. EEG data was imported into Matlab, and band-pass filtered between (3-35 Hz) to  
56  
57 remove artefacts present in the signal due to the MF exposure at 50 Hz. Importantly, the entire  
58  
59  
60

1  
2  
3 experiment was also performed using a phantom (watermelon) with the EEG cap that was  
4  
5 setup in the exact same manner than with participants, to validate the pre-processing step.  
6  
7 More specifically, the same EEG cap than the one used in the experimental human study was  
8  
9 put on a watermelon, and all electrodes were filled with electrolyte to decrease impedance, as  
10  
11 done in actual participants. Two thin wires were inserted in the watermelon, and connected to  
12  
13 a current generator to apply a constant current at 10 Hz (alpha frequency), with an intensity  
14  
15 calibrated to generate a detectable current at the EEG electrode level of approx. 50  
16  
17 microvolts, i.e. an amplitude comparable to an actual EEG. This provided us with a “ground  
18  
19 truth” EEG to test if the processing pipeline removing MF exposure artefacts was altering the  
20  
21 actual EEG. Then, the watermelon was setup in the MF exposure device, and the entire MF  
22  
23 exposure protocol was ran. The acquired EEG was then filtered and we verified that the  
24  
25 artefact-free reconstructed EEG was identical to the ground truth EEG, confirming that our  
26  
27 processing pipeline was not altering the EEG and not biasing further connectivity analyses.  
28  
29  
30  
31  
32

33 For each EEG recording, the 55 EEG epochs (11 MF exposure conditions, each  
34  
35 repeated 5 times) were extracted and imported in the Brainstorm Matlab package (Tadel et al.,  
36  
37 2011). The entire duration (5 seconds) of each epoch was extracted, and a window function  
38  
39 was applied (Hamming window) to avoid edge effects.  
40  
41

42 Nasion-inion and preauricular anatomical measurements were made to locate each  
43  
44 individual’s vertex site. Electrode impedances were kept below 10 kOhm. EEG signals are  
45  
46 frequently contaminated by several artifacts sources, which were addressed using the same  
47  
48 preprocessing steps as described in several previous studies dealing with EEG resting-state  
49  
50 data (Kabbara et al., 2017; Kabbara et al., 2018). Briefly, bad channels (signals that are either  
51  
52 completely flat or contaminated by movement artifacts) were identified by visual inspection,  
53  
54 complemented by the power spectral density. These bad channels were then recuperated using  
55  
56 an interpolation procedure implemented in Brainstorm (Tadel et al., 2011), using neighboring  
57  
58  
59  
60

1  
2  
3 electrodes within a 5 cm radius. Epochs with voltage fluctuations  $> +80 \mu\text{V}$  and  $< -80 \mu\text{V}$   
4  
5 were removed.  
6  
7  
8  
9

### 10 *Magnetophosphenes reports*

11  
12 Subjects were instructed to report magnetophosphenes perception by using a button  
13  
14 press as soon as they could when the perception began. Subjects were instructed to press only  
15  
16 once, however a custom Matlab code was developed to detect and remove possible “double  
17  
18 presses” which could accidentally occur.  
19  
20  
21  
22  
23  
24  
25

### 26 *Brain networks reconstruction*

27  
28 Functional brain networks were reconstructed using the EEG source-space  
29  
30 connectivity method (Hassan et al., 2014; Hassan and Wendling, 2018), which includes two  
31  
32 main steps: 1) reconstruct dynamics of the cortical sources by solving the inverse problem,  
33  
34 and 2) measure the statistical couplings (functional connectivity) between the regional time  
35  
36 series. The EEG source connectivity method links the recorded scalp EEG signals with the  
37  
38 functional relationships between anatomical brain regions (e.g., networks), through the EEG  
39  
40 inverse problem that provides the localization of the cortical sources originating these EEG  
41  
42 signals. Several methods exist for both of these two steps (EEG inverse problem and  
43  
44 functional connectivity measures). Here, we used the weighted minimum norm estimate  
45  
46 (wMNE) algorithm as an inverse solution. The reconstructed regional time series were filtered  
47  
48 in different frequency bands (theta, 4-7 Hz; alpha, 8-12 Hz; beta; 13-30 Hz). For each  
49  
50 frequency band, functional connectivity was computed between the regional time series using  
51  
52 the phase locking value (PLV) measure (Lachaux et al., 1999). The wMNE/PLV combination  
53  
54  
55  
56  
57  
58  
59  
60

1  
2  
3 was chosen according to recent model-based and data-driven comparative studies of different  
4  
5 inverse/connectivity combinations (Hassan et al., 2017).  
6  
7  
8  
9

10 EEGs and structural MRI template (ICBM152) were co-registered through the  
11 identification of anatomical markers using Brainstorm (Tadel et al., 2011). A Desikan-  
12 Killiany atlas-based segmentation approach was used, consisting in 68 cortical regions  
13  
14 (Desikan et al., 2006). The OpenMEEG (Gramfort et al., 2010) software was used to compute  
15  
16 the three-layer (scalp, skull and brain) model. The functional connectivity between the 68  
17  
18 regional time series was computed using the PLV, using EEGNET (Hassan et al., 2015; Tadel  
19  
20 et al., 2011), for each condition, in the different frequency bands. This resulted for each  
21  
22 subject, in each of the three frequency bands, in 55 68x68 connectivity matrices (one per MF  
23  
24 condition). Finally, we only kept the strongest 10% of connections (proportional threshold).  
25  
26  
27  
28  
29  
30  
31  
32

### 33 *Characterization of functional networks*

34  
35 Our main objective was to explore two important properties related to information  
36  
37 processing in the human brain network:  
38  
39

40 - **Network segregation**, which reflects local information processing. For this reason,  
41  
42 the clustering coefficient 'Cc' was computed, considered as a direct measure of network  
43  
44 segregation (Bullmore and Sporns, 2009). In brief, Cc represents how close a node's  
45  
46 neighbors tend to cluster together (Watts and Strogatz, 1998). This coefficient is the  
47  
48 proportion of connections among a node's neighbors, divided by the number of connections  
49  
50 that could possibly exist between them, which is 0 if no connections exist and 1 if all  
51  
52 neighbors are connected.  
53  
54

55  
56 - **Network integration**, which reflects global information processing. The  
57  
58 participation coefficient was computed to measure the diversity of node inter-modular  
59  
60

1  
2  
3 connections (Guimera and Amaral, 2005). The participation coefficient ( $P_c$ ) of a node is close  
4  
5 to 1 if its links are uniformly distributed among all the modules and 0 if all of its links are  
6  
7 within its own module. Nodes with high participation coefficients interconnect multiple  
8  
9 modules together, and hence can be seen as connectivity hubs. At the group level, this  
10  
11 resulted in a  $C_c$  and  $P_c$  matrix for each of the 68 ROIs in each of the 55 MF conditions, for  
12  
13 each frequency band.  
14  
15

16  
17 We have chosen to focus on those two graph metrics, clustering and participation for the  
18  
19 reason that, many different metrics exist, and one cannot simply apply all of them to identify  
20  
21 one that is significant. Therefore, we have rather chosen to use specific metrics that are  
22  
23 directly linked with the hypothesis being tested. Since two of the main theories of  
24  
25 consciousness, namely the Global Workspace Theory (GWT) and the Integrated Information  
26  
27 Theory (IIT), explicitly emphasize the role of integration/distant processing, we have chosen  
28  
29 to use the participation coefficient that quantifies the connectivity between distant  
30  
31 regions/modules. Furthermore, the concept of differentiation is linked with the clustering  
32  
33 coefficient, and is another key concept in terms of the neuronal processes associated with  
34  
35 consciousness (Koch et al., 2016). Consequently, we have focused in this study exclusively  
36  
37 on the parameters of clustering and participation that are directly linked with the question  
38  
39 addressed and its conceptual framework, i.e. the maintenance of conscious processes through  
40  
41 long-distance communication between brain regions.  
42  
43  
44  
45

#### 46 47 *Statistical analysis*

48  
49 First, the Pearson correlation between the  $C_c/P_c$  matrix and the reported perception  
50  
51 curve (probability of perception between 0 and 1, computed for each condition as the number  
52  
53 of button presses divided by the number of repetitions, i.e. 5) was computed using Matlab and  
54  
55 the False-Detection Rate (FDR) method was used to account for multiple comparisons. In this  
56  
57 paper, we used the Benjamini and Hochberg (B-H) procedure, see (Thissen et al., 2002)  
58  
59  
60

1  
2  
3 which consists in adapting the new threshold to each resultant p-value instead of using the  
4 same threshold as suggested in Bonferroni correction. The graph theoretical metrics were  
5 computed using the Brain Connectivity Toolbox (Rubinov and Sporns, 2010). Second, the  
6 linear trend associated with increasing MF flux density was assessed using the Jonckheere-  
7 Terpstra test (implemented in Matlab, The Mathworks, USA) with correction of the  
8 significance threshold using the FDR. The correlation with the (non-linear) perception curve  
9 was assessed using a linear correlation (Matlab, The Mathworks, USA) corrected using FDR.  
10  
11  
12  
13  
14  
15  
16  
17  
18  
19  
20

### 21 *Quantification of the ignition process*

22  
23 To quantify the ignition process, the functional connectivity matrices were averaged  
24 over subjects at each flux density value (averaged also over five trials). The degree of each  
25 brain region, i.e. its number of functional connections, was then computed (after keeping the  
26 highest 50% of connections, keeping in mind that this threshold was used to estimate the  
27 connections with the highest degree, and not the strongest connections, for which a  
28 proportional threshold of 10% was used as aforementioned). The ignition process is therefore  
29 considered as the increased number of functional long-range connections when the probability  
30 of perception increases.  
31  
32  
33  
34  
35  
36  
37  
38  
39  
40  
41  
42  
43  
44

### 45 *Software*

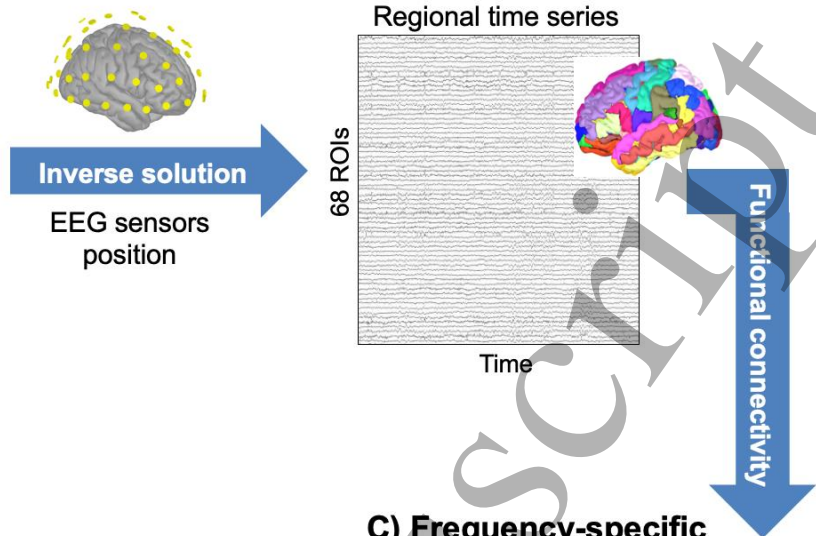
46 The functional connectivity, network measures and network visualization were  
47 performed using BCT (Rubinov and Sporns, 2010), EEGNET (Hassan et al., 2015) and  
48 BrainNet viewer (Xia et al., 2013), respectively.  
49  
50  
51  
52  
53

54 The study design is summarized in Figure 1 below.  
55  
56  
57  
58  
59  
60

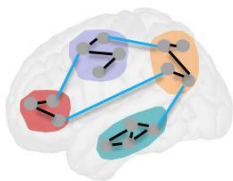
**A) Data recordings:  
MF exposure + dense EEG**



**B) Reconstruction of brain sources**



**D) Metrics of network  
integration and segregation**



**C) Frequency-specific  
functional brain networks**

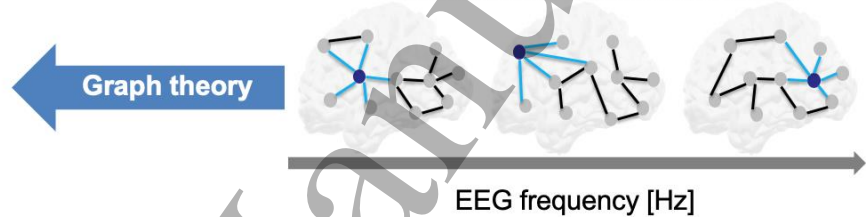


**Fig. 1. Study design and data analysis pipeline.** **A)** MF exposure setup (water-cooled Helmholtz coils, in-house design and engineering, see Methods for details) used to induce magnetophosphene perception. Subjects could report magnetophosphene perception using a button press. Dense-EEG (64 channels, MRI compatible cap) was recorded throughout the entire experiment. Informed consent of the study participant was obtained for the publication of this picture in an online open-access publication. **B)** Source activity was reconstructed for the 68 regions of the Desikan-Killiany atlas. **C)** Frequency-specific functional networks were computed for the theta, alpha and beta frequency bands. **D)** Metrics from graph theory were used to quantify segregation and integration (local and global processing, using clustering and participation coefficients, respectively).

## Results

As expected, participants did not perceive phosphenes in the sham condition (0 mT), as seen in Fig. 2, and the perception of magnetophosphenes, as assessed by perception button-press self-reports, began with a 0.28 probability of perception at a threshold value of 20 mT when the entire head was stimulated by the homogeneous 50 Hz sinusoidal signal. It is worth noting that, at the maximal MF flux density value used (50 mT), the probability of magnetophosphene perception was close to 1 (0.96). Phosphene perception was reported by all subjects as colorless, stroboscopic dots/lines. The resulting magnetophosphene perception curve as a function of the MF flux density results in a sigmoid-like function, as can be seen in Fig. 2 (lower panel), similarly to the curve obtained in monkeys with increasing intracranial stimulation current values (van Vugt et al., 2018). The comparison between these two curves is direct: intracranial current injection results in an electric field that depolarizes neighboring neuronal elements, while MF exposure also induces an electric field in brain tissue per Maxwell-Ampere's law of magnetic induction. One difference is that, in the present study, retinal cells instead of visual cortex cells are modulated by the induced electric field. As detailed in the Methods section, each functional network reconstructed in each of the 55 conditions featured 68 ROIs, and the participation and clustering coefficients quantifying *integration* (global) and *segregation* (local) processing respectively, were computed for each frequency band (theta, 4-7 Hz; alpha, 8-12 Hz; beta, 13-30 Hz). Gamma-band networks were not estimated due to the need of filtering the EEG from 50 Hz stimulation contamination, and to avoid possible biases. In the following, all *p*-values were corrected for multiple comparisons using the False Detection Rate (FDR) method.

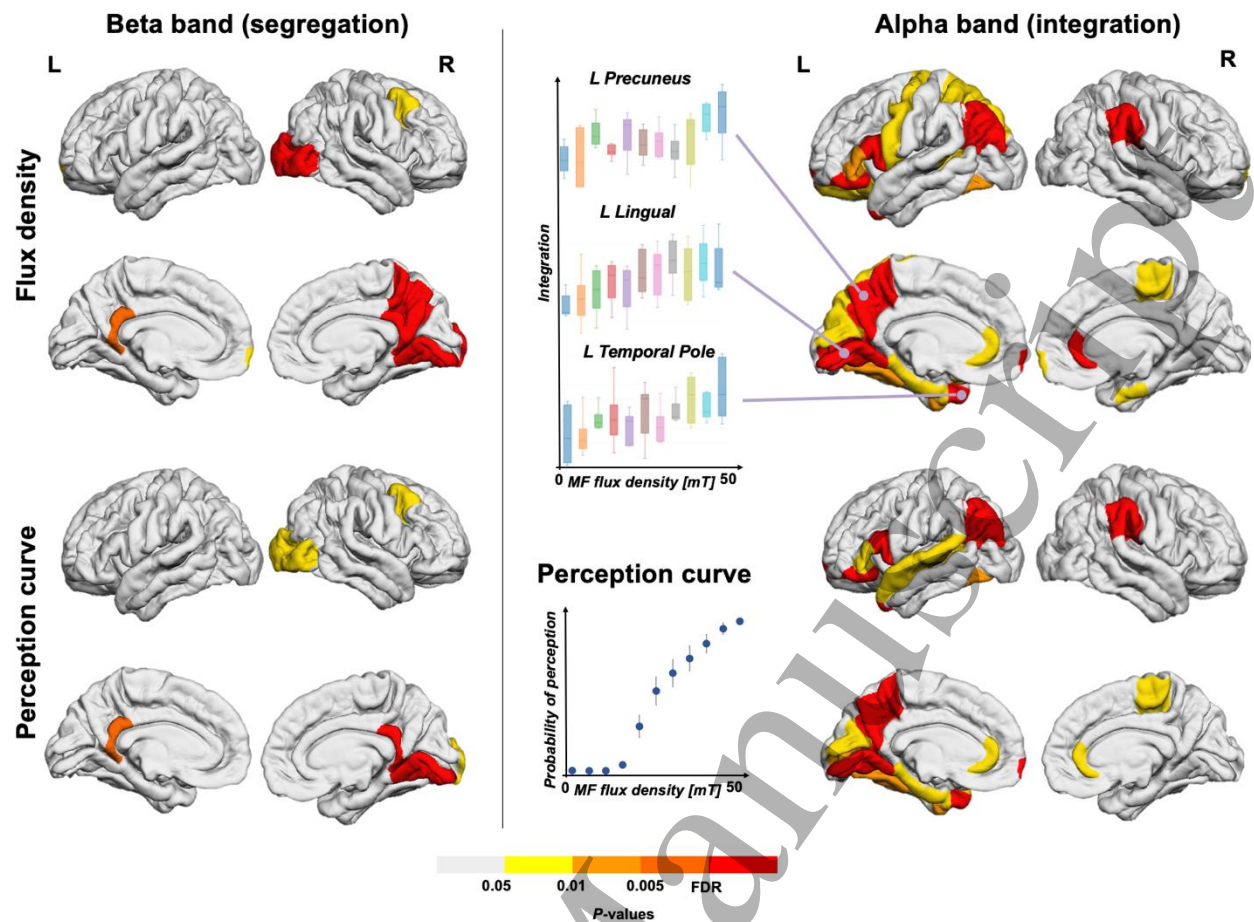


**Fig. 2. Left panel.** Segregation results in the beta-band functional network (linear trend, flux density sub-panel; correlated with perception reports, perception curve sub-panel). Results are presented for each hemisphere. **Right panel.** Integration results in the alpha-band functional network (linear trend, flux density sub-panel; correlated with perception reports, perception curve sub-panel). Results are presented for each hemisphere. The increase in integration with flux density is shown for three regions of interest (left precuneus, left lingual and left temporal pole), along with the perception probability curve for magnetophosphene from subjective reports (N=20 subjects).

First, brain structures for which integration (quantified by the participation coefficient (Guimera and Nunes Amaral, 2005)) was correlated with the MF flux density were almost exclusively within the alpha band (see Fig. 2, right panel). More specifically, there were

1  
2  
3 structures involved both in “subliminal” (i.e., 50 Hz MF exposure below the perception  
4 threshold) and suprathreshold magnetophosphene perception. These regions involved DMN  
5 (Default Mode Network) structures such as the right rostral anterior cingulate ( $p=0.0012$ ) and  
6 left parahippocampal gyrus ( $p=0.0116$ ); a structure from the VIS (visual) network (left  
7 fusiform,  $p=0.0089$ ); and a DAN (Default Attention Network) structure (left pars triangularis,  
8  $p=0.007$ ). The left pericalcarine cortex ( $p=0.0052$ , visual cortex area), right entorhinal  
9 ( $p=0.0085$ ), right frontal pole ( $p=0.0085$ ), and right paracentral ( $p=0.0092$ ) were also involved.

10  
11  
12  
13  
14  
15  
16  
17  
18  
19 Regions correlating specifically with the perception curve involved a DMN region (left  
20 precuneus,  $p=0.001$ ), two regions from the DAN (left pars orbitalis and left pars opercularis,  
21  $p<0.001$ ), and a region from the SAN (Salience Attention Network), namely the right  
22 supramarginal gyrus ( $p<0.001$ ). Interestingly, the right supramarginal gyrus has been  
23 previously identified as involved in phosphene perception in humans using intracranial  
24 stimulation (Beauchamp et al., 2012). The left temporal pole,  $p < 0.001$ , the left frontal pole,  
25  $p=0.0026$  and left inferior parietal,  $p<0.001$  were also involved.

26  
27  
28  
29  
30  
31  
32  
33  
34  
35  
36  
37  
38  
39  
40  
41  
42  
43  
44  
45  
46  
47  
48  
49  
50  
51  
52  
53  
54  
55  
56  
57  
58  
59  
60  
Second, magnetophosphene perception was associated with an increase in segregation  
(local processing) almost exclusively in a beta functional network, as illustrated in Fig. 2 (left  
panel). More specifically, the network segregation increased (both for “subliminal” and  
conscious perception) in the right lingual cortex ( $p<0.001$ , VIS), within DMN regions (right  
precuneus,  $p=0.0018$ ; and left/right isthmus cingulate,  $p=0.0019$  and  $p<0.001$  respectively)  
and a DAN region (right caudal middle frontal gyrus,  $p=0.0031$ ). In the case of conscious  
(suprathreshold) perception, only the right lingual cortex and right isthmus cingulate ( $p <$   
 $0.001$ ) specifically showed significant correlation with the perception curve in terms of beta  
network segregation.

1  
2  
3 Notably, while magnetophosphene perception was mainly restricted to effects within  
4  
5 alpha- and beta-band functional networks, a limited number of brain structures displayed  
6  
7 increased integration within the theta (left pars triangularis,  $p < 0.001$ ; right middle temporal,  
8  
9  $p = 0.001$ ) and beta (left precuneus,  $p < 0.001$ ) bands. Furthermore, regarding network  
10  
11 segregation, an effect was also identified in a single region (right superior frontal gyrus,  
12  
13  $p < 0.001$ ) of the alpha functional network. It should also be noted that there was an asymmetry  
14  
15 between hemispheres in terms of regions involved. This is consistent, for example, with the  
16  
17 known hemispheric specialization of occipito-temporal pathways depending on the spatial  
18  
19 resolution of visual stimuli (Kauffmann et al., 2014).  
20  
21  
22  
23

24  
25 In addition, we also compared how integration and segregation varied when the  
26  
27 stimulus (MF) was kept constant, but conscious awareness was different (report versus no  
28  
29 report). This was done both at the individual- and group-levels. For the individual level, we  
30  
31 used for each subject the condition that was associated with a probability of perception as  
32  
33 close as possible to 50% (either 2 or 3 perceptions out of 5 repetitions). For the group level,  
34  
35 the 25 mT condition was retained since it was associated with a mean perception probability  
36  
37 of 54%. In both analyses, the participation and clustering coefficient for “seen” epochs versus  
38  
39 “unseen” epochs were compared for each ROI, including a FDR correction for multiple  
40  
41 comparisons. Using individual perception thresholds, only one region had increased  
42  
43 integration in the “seen” condition (right orbitofrontal cortex,  $p = 0.0001$ ), and in the theta  
44  
45 band only. No ROI had significantly different clustering coefficients. When using the group  
46  
47 perception threshold of 25 mT, no ROI had significantly integration in any frequency band,  
48  
49 while two ROIs had a significantly different clustering coefficient in “seen” versus “unseen”  
50  
51 epochs: right superior parietal cortex ( $p < 0.0004$ ) and the left pars orbitalis ( $p = 0.0012$ ).  
52  
53  
54  
55

56  
57 Finally, we deciphered the ignition process during the conscious perception of  
58  
59 magnetophosphenes (Fig. 3) during increased MF flux density, corresponding to a higher  
60

level of retinal stimulation. In this example, the number of functional connections of the left precuneus (one of the regions achieving the highest significance regarding integration in the alpha band) to distant regions, including frontal regions, increases with the probability of perception.

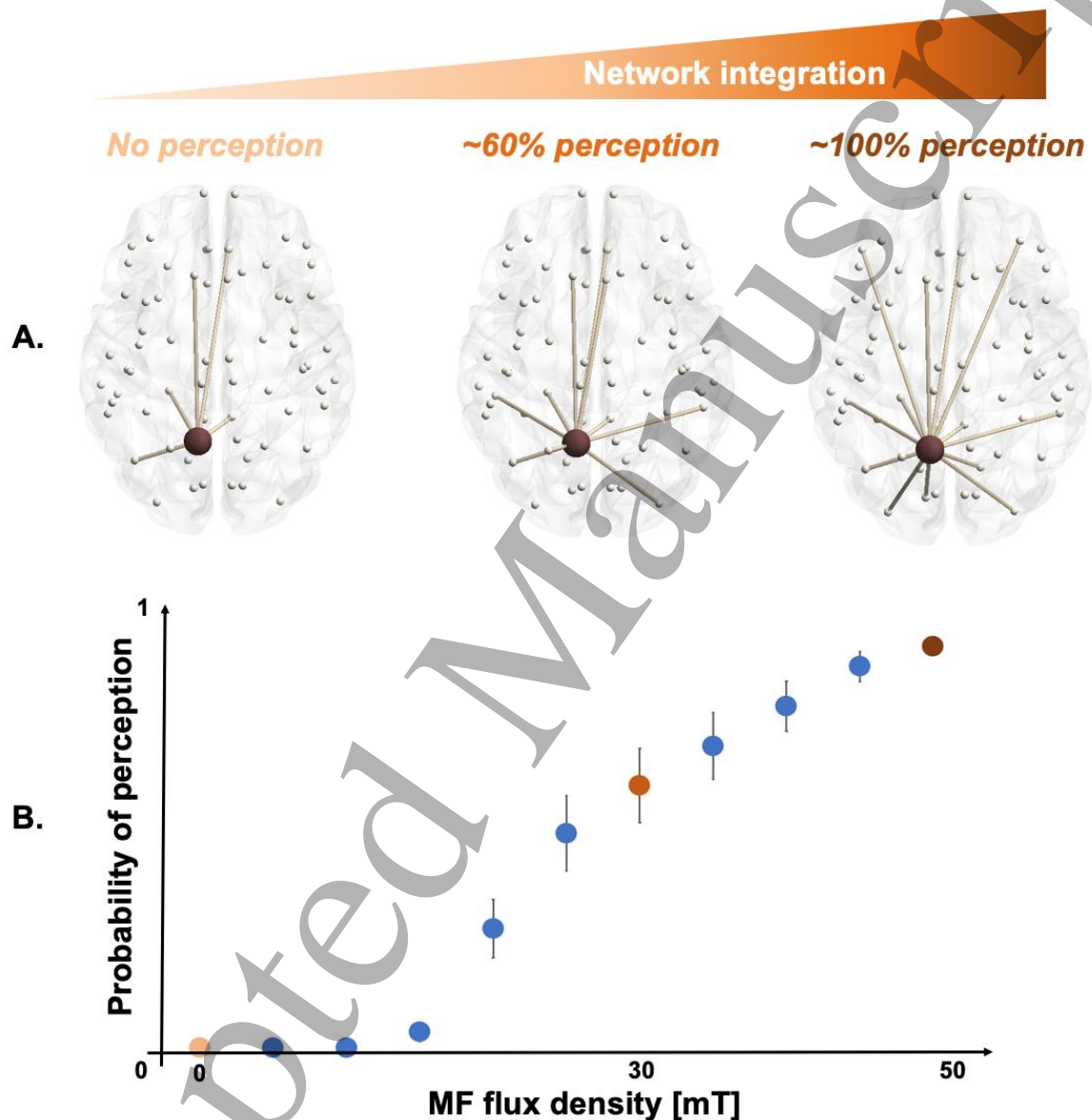


**Fig. 3.** **A.** Illustration of the ignition process occurring with the increase of long-range connections (in this example, from the left precuneus) associated with the increase in probability of magnetophosphene perception at 0 mT (left), 30 mT (middle) and 50 mT (right). **B.** Probability of magnetophosphene perception curve from the N=20 subjects

1  
2  
3 between 0 and 50 mT, with the 0 (light orange), 30 (orange) and 50 mT (burgundy) points  
4 highlighted.  
5  
6  
7  
8  
9

10  
11  
12  
13  
14 This drastic increase in the functional connections between the left precuneus (a  
15 critical region from the DMN) and distant regions emphasize the central role of long-range  
16 connectivity for the emergence of conscious perception. Interestingly, long-range functional  
17 connections at baseline (without perception) remain present when the perception probability  
18 increases, while novel long-range connections gradually appear. Here, we have focused this  
19 figure on the left precuneus, since this region was one of the most significantly correlated  
20 with conscious perception in terms of integration within the alpha band. Furthermore, the  
21 precuneus has been shown to be central in several studies of patients suffering from disorders  
22 of consciousness. For example, it has been shown that an hypo-metabolism within the  
23 precuneus was observed in Unresponsive Wakefulness Syndrome (Annen et al., 2016), and  
24 that an increase in metabolism was observed within this region after emergence from  
25 Minimally Conscious States (Laureys et al., 2006).  
26  
27  
28  
29  
30  
31  
32  
33  
34  
35  
36  
37  
38  
39  
40  
41  
42  
43

#### 44 **Discussion**

45  
46 Magnetophosphene perception increases as a function of the increasing level of  
47 magnetic stimulation, which results from the induced electric fields modulating retinal neuron  
48 signaling (Attwell, 2003). The increase in magnetophosphene perception probability induced  
49 in healthy human volunteers results in an increase of information integration at the brain-scale  
50 in the alpha band. Conscious perception was tracked using participant subjective reports and  
51 increased with gradually increasing stimulus strength. The frequency-dependent increase of  
52 information integration was observed mostly in visual- and DMN-related regions, and also in  
53  
54  
55  
56  
57  
58  
59  
60

1  
2  
3 a few frontal regions. We also identified an increase in the number of functional connections  
4  
5 mostly in the alpha band between one of the most critical nodes of the identified cortical  
6  
7 network, namely the left precuneus, and distant regions, when the probability of perception  
8  
9 increased. To our knowledge, this is the first use of EEG source-space networks to  
10  
11 characterize the increase of integration information as a consequence of conscious visual  
12  
13 perception. These results are in line with the recent study by van Vugt et al. (van Vugt et al.,  
14  
15 2018) who identified the ignition process in monkeys, also using a phosphene perception  
16  
17 paradigm (with stimulation delivered intracranially, as opposed to non-invasively in the  
18  
19 present study). Taken together, these results provide further support for the ignition process  
20  
21 that was conceptualized in GWT, and also for the integration concept at the core of IIT. While  
22  
23 our results did not provide a definite illustration of the ignition process in humans during  
24  
25 conscious perception, our results obtained through the EEG source connectivity technique  
26  
27 hint at this process. In order to obtain a more definite answer, possibilities include performing  
28  
29 a larger number of repetitions per condition at the individual perception threshold, and/or  
30  
31 increasing the sample size. Taken together, our results suggest an increase of integration  
32  
33 during conscious perception in a limited number of brain regions, in low-frequency rhythms  
34  
35 (theta, alpha). This is in line with our recent proposal that low-frequency rhythms enable the  
36  
37 “locking” between distant brain regions, while higher-frequency rhythms (generated more  
38  
39 locally) are involved in information transfer itself (Modolo et al., 2020).

40  
41  
42 Interestingly, changes in integration (quantified using the participation coefficient) were  
43  
44 mostly within low-frequency bands (theta, alpha), while changes in segregation (quantified  
45  
46 using the clustering coefficient) were mostly within a higher-frequency band (beta). This  
47  
48 supports the idea that low-frequency oscillations such as theta and alpha are involved  
49  
50 establishing transient communication between distant brain regions and shaping the global  
51  
52 architecture of functional networks (e.g., Gating by Inhibition, see (Bonfond et al., 2017),  
53  
54  
55  
56  
57  
58  
59  
60

1  
2  
3 and review in (Modolo et al., 2020)), while high-frequency rhythms are rather involved in the  
4  
5 processing of information, an example being communication through coherence (CTC, (Fries,  
6  
7 2005)). Consequently, our results pertaining to conscious perception support this general view  
8  
9 about the general function of neuronal oscillations in terms of establishing and activating  
10  
11 transient functional networks in general, and in conscious process in particular. Another  
12  
13 originality of this study is that we characterized the functional networks involved in the  
14  
15 biological effect occurring at the lowest known level of *in situ* electric field, which may  
16  
17 provide further arguments for the use of magnetophosphene perception to define international  
18  
19 safety electromagnetic exposure guidelines (IEEE, 2010; International Commission on Non-  
20  
21 Ionizing Radiation, 2010).  
22  
23  
24

25  
26 One limitation of our approach is the use of EEG source reconstruction, which is not  
27  
28 free of biases. Numerous different methods have been indeed proposed to reconstruct source-  
29  
30 level activity from EEG (scalp) signals and differ by their hypotheses regarding the spatial  
31  
32 extent or number of sources, for example. Therefore, it is not surprising that those algorithms  
33  
34 can result in slightly different estimations of the underlying cortical sources [Mahjoory et al.,  
35  
36 2017]. It has also been shown that connectivity measures can provide indeed quite different  
37  
38 estimates [Mahjoory et al., 2017], which has to be kept in mind when selecting measures of  
39  
40 functional connectivity. In this paper, we have used the wMNE source reconstruction method,  
41  
42 that was shown to provide when used in combination with PLV the best estimation of ground  
43  
44 truth cortical sources [Hassan et al., 2013]. Finally, one should be cautious about comparing  
45  
46 those EEG-based results with fMRI studies, since the relationship between the BOLD signal  
47  
48 and EEG signals in specific frequency bands is highly complex, as discussed in [Scheeringa et  
49  
50 al., 2016].  
51  
52  
53

54  
55 Another limitation in our study is that the whole brain was exposed to the delivered MF,  
56  
57 which leaves open the possibility that some identified brain regions were not necessarily  
58  
59  
60

1  
2  
3 associated with phosphene perception, but rather with neuromodulation from the MF. Our  
4  
5 whole head exposure protocol was chosen since it is the most effective to generate  
6  
7 phosphenes perception non-invasively, which was the most important required feature at this  
8  
9 initial stage of evaluating if brain networks would react to this perception. The MF exposure  
10  
11 device was very different from a TMS (transcranial magnetic stimulation) device in the  
12  
13 following respects: 1) the resulting MF flux density was much lower (0.05 T here versus > 1  
14  
15 T for TMS devices); 2) the level of dB/dt (proportional to the current induced in brain tissue)  
16  
17 was much lower (approx. 15 T/s here versus > 10,000 T/s for TMS devices); 3) TMS targets a  
18  
19 relatively narrow brain region typically at spiking suprathreshold levels, while the present  
20  
21 exposure device provides whole-brain exposure at subthreshold levels (no neuronal firing  
22  
23 outside of the retina can be directly induced by the MF used in this study even at the highest  
24  
25 flux density -50 mT-, as detailed below); 4) TMS uses very short pulses (typically 100  $\mu$ s)  
26  
27 while the present MF exposure can deliver MF during minutes continuously. Next  
28  
29 developments will use a more focal stimulus targeting the eyeball. Let us mention that the MF  
30  
31 stimulation device used in this study was originally designed and built to study non-invasive  
32  
33 neuromodulation thresholds inducing systematic acute responses in humans for the purpose of  
34  
35 documenting international guidelines and standards regarding human electromagnetic field  
36  
37 exposure. The main advantage of this non-invasive stimulation modality applied to the visual  
38  
39 system is that the stimulus can be delivered even in an apparently unconscious patient with  
40  
41 the eyes closed, to whom it would not be possible to present stimuli on a screen. For these  
42  
43 reasons, and because brain functions associated with conscious visual awareness are well  
44  
45 studied and well understood, better than for auditory awareness (acknowledged for example  
46  
47 by (Snyder et al., 2012)), we chose to study how the circuits of visual perception would  
48  
49 respond to such stimulation of visual pathways.  
50  
51  
52  
53  
54  
55  
56  
57  
58  
59  
60

1  
2  
3 That being said, one critical point is that the levels of MF flux density in this study,  
4 and delivered during such short durations (5 seconds), are known to *activate the retina only*,  
5 since the perception of magnetophosphenes is the biological effect occurring at the lowest  
6 known MF flux density: it is precisely for this reason that the international guidelines  
7 protecting the general public and workers from the adverse effects from electromagnetic  
8 fields exposure are based, for extremely low-frequency fields (< 300 Hz), on the perception of  
9 magnetophosphenes (IEEE, 2010; International Commission on Non-Ionizing Radiation,  
10 2010). Therefore, from the existing literature, direct acute effects of the MF delivered here on  
11 another system than the retina, is, according to the current existing literature, extremely  
12 unlikely. This supports further that the observed changes in functional connectivity are indeed  
13 associated with the perception of magnetophosphenes. Another limitation is that, since we  
14 used a 50 Hz stimulus, we were not able to investigate gamma-band functional networks. A  
15 50 Hz frequency was selected because it is reported to be effective in triggering phosphene  
16 perception (phosphene perception decreases as the stimulus frequency increases), although  
17 the related contamination of EEG signals involves filtering and thereby prevents investigation  
18 of gamma-related processes.  
19  
20  
21  
22  
23  
24  
25  
26  
27  
28  
29  
30  
31  
32  
33  
34  
35  
36  
37  
38

39  
40 In addition to a contribution in terms of the fundamental mechanisms of  
41 consciousness, we also suggest that our experimental paradigm could form the basis of a  
42 novel protocol to probe conscious processes in humans. While a rather cumbersome  
43 experimental setup was used in this study, it would be possible to simplify it by using scalp  
44 (surface) electrodes placed on the temples and with an adapted level of delivered electrical  
45 current. One could also argue that a more conventional visual stimulation at different  
46 intensities could be used, avoiding the complications linked with the use of brain stimulation.  
47 However, we have in mind the potential to use integration as a possible measure of residual  
48 conscious processes, for example in minimally conscious patients. In those patients, blindness  
49  
50  
51  
52  
53  
54  
55  
56  
57  
58  
59  
60

1  
2  
3 can occur due to cornea dryness, preventing the use of classical stimulation protocols. Since  
4  
5 magnetic stimulation bypasses the cornea and directly impacts the retina, such issue would  
6  
7 not occur with our method, opening the possibility to develop neuromodulation-based  
8  
9 protocols of consciousness evaluation while requiring considerable less power than existing  
10  
11 TMS protocols. Furthermore, this work identifies a key brain region in the conscious  
12  
13 perception of a visual stimulus, namely the precuneus, a brain region that has been shown to  
14  
15 be key for the maintenance of consciousness (Cavanna and Trimble, 2006). Hence, our results  
16  
17 bring support for a role of the precuneus not only in “basal” consciousness, but also in the  
18  
19 perception of external stimuli (conscious perception).  
20  
21  
22

23  
24 Another more fundamental implication of these results is that the spatial extent of  
25  
26 functional network dynamics and frequency processing is frequency dependent: during  
27  
28 magnetophosphene perception, distant information processing increases mostly within the  
29  
30 alpha band, while local information processing increases mostly within the beta band. This  
31  
32 result is consistent with other studies pointing to the role of low-frequency oscillations for  
33  
34 distant communication between brain regions, while higher frequency rhythms would rather  
35  
36 contribute to stimulus encoding itself (Lisman and Jensen, 2013). Therefore, our results bring  
37  
38 further support to the framework conceptualizing information flow and processing between  
39  
40 brain structures as an interplay between slow and fast oscillations, each associated with a  
41  
42 “range” for information processing and a specific functional role.  
43  
44  
45

46  
47 **Conflicts of interest:** The authors have no competing financial or non-financial interests to  
48  
49 declare.  
50

## 51 52 **References and Notes**

53  
54  
55 Annen, J., et al., 2016. Function-structure connectivity in patients with severe brain injury as  
56 measured by MRI-DWI and FDG-PET. *Hum Brain Mapp.* 37, 3707-3720.  
57  
58 Attwell, D., 2003. Interaction of low frequency electric fields with the nervous system: the  
59 retina as a model system. *Radiat Prot Dosimetry.* 106, 341-8.  
60

- 1  
2  
3 Beauchamp, M.S., et al., 2012. Electrocorticography links human temporoparietal junction to  
4 visual perception. *Nat Neurosci.* 15, 957-9.  
5 Bonnefond, M., Kastner, S., Jensen, O., 2017. Communication between brain areas based on  
6 nested oscillations. *eNeuro.* 4, 0153-16.  
7 Bullmore, E., Sporns, O., 2009. Complex brain networks: graph theoretical analysis of  
8 structural and functional systems. *Nat Rev Neurosci.* 10, 186-98.  
9 Casali, A.G., et al., 2013. A theoretically based index of consciousness independent of  
10 sensory processing and behavior. *Sci Transl Med.* 5, 198ra105.  
11 Cavanna, A.E., Trimble, M.R., 2006. The precuneus: a review of its functional anatomy and  
12 behavioural correlates. *Brain.* 129, 564-83.  
13 Dehaene, S., Kerszberg, M., Changeux, J.P., 1998. A neuronal model of a global workspace  
14 in effortful cognitive tasks. *Proc Natl Acad Sci U S A.* 95, 14529-34.  
15 Dehaene, S., et al., 2001. Cerebral mechanisms of word masking and unconscious repetition  
16 priming. *Nat Neurosci.* 4, 752-8.  
17 Dehaene, S., et al., 2006. Conscious, preconscious, and subliminal processing: a testable  
18 taxonomy. *Trends Cogn Sci.* 10, 204-11.  
19 Dehaene, S., Changeux, J.P., 2011. Experimental and theoretical approaches to conscious  
20 processing. *Neuron.* 70, 200-27.  
21 Desikan, R.S., et al., 2006. An automated labeling system for subdividing the human cerebral  
22 cortex on MRI scans into gyral based regions of interest. *Neuroimage.* 31, 968-80.  
23 Fries, P., 2005. A mechanism for cognitive dynamics: neuronal communication through  
24 neuronal coherence. *Trends Cogn Sci.* 9, 474-80.  
25 Gramfort, A., et al., 2010. OpenMEEG: open-source software for quasistatic  
26 bioelectromagnetics. *Biomed Eng Online.* 9, 45.  
27 Gross, J., et al., 2004. Modulation of long-range neural synchrony reflects temporal  
28 limitations of visual attention in humans. *Proc Natl Acad Sci U S A.* 101, 13050-5.  
29 Guimera, R., Amaral, L.A., 2005. Cartography of complex networks: modules and universal  
30 roles. *J Stat Mech.* 2005, nihpa35573.  
31 Guimera, R., Nunes Amaral, L.A., 2005. Functional cartography of complex metabolic  
32 networks. *Nature.* 433, 895-900.  
33 Harnad, S., 1998. Explaining consciousness: the hard problem. *Trends Cogn Sci.* 2, 234-5.  
34 Hassan, M., et al., 2014. EEG source connectivity analysis: from dense array recordings to  
35 brain networks. *PLoS One.* 9, e105041.  
36 Hassan, M., et al., 2015. EEGNET: An Open Source Tool for Analyzing and Visualizing  
37 M/EEG Connectome. *PLoS One.* 10, e0138297.  
38 Hassan, M., et al., 2017. Identification of Interictal Epileptic Networks from Dense-EEG.  
39 *Brain Topogr.* 30, 60-76.  
40 Hassan, M., Wendling, F., 2018. Electroencephalography Source Connectivity: Aiming for  
41 High Resolution of Brain Networks in Time and Space. *IEEE Signal Processing Magazine.*  
42 35, 81-96.  
43 IEEE, 2010. IEEE Recommended Practice for Measurements and Computations of Electric,  
44 Magnetic, and Electromagnetic Fields with Respect to Human Exposure to Such Fields, 0 Hz  
45 to 100 kHz. *IEEE Std C95.3.1-2010.*  
46 International Commission on Non-Ionizing Radiation, P., 2010. Guidelines for limiting  
47 exposure to time-varying electric and magnetic fields (1 Hz to 100 kHz). *Health Phys.* 99,  
48 818-36.  
49 Kabbara, A., et al., 2017. The dynamic functional core network of the human brain at rest. *Sci*  
50 *Rep.* 7, 2936.  
51 Kabbara, A., et al., 2018. Reduced integration and improved segregation of functional brain  
52 networks in Alzheimer's disease. *J Neural Eng.* 15, 026023.  
53  
54  
55  
56  
57  
58  
59  
60

- 1  
2  
3 Kauffmann, L., Ramanoel, S., Peyrin, C., 2014. The neural bases of spatial frequency  
4 processing during scene perception. *Front Integr Neurosci.* 8, 37.  
5 Keenlside, L.D., et al., 2013. Creating an ELF magnetic field system over 50 mT for human  
6 whole head threshold studies. Proceedings of the BioEM2015 conference (Annual Joint  
7 Meeting of the Bioelectromagnetics Society and the European Bioelectromagnetics  
8 Association).  
9 Koch, C., et al., 2016. Neural correlates of consciousness: progress and problems. *Nat Rev  
10 Neurosci.* 17, 307-21.  
11 Lachaux, J.P., et al., 1999. Measuring phase synchrony in brain signals. *Hum Brain Mapp.* 8,  
12 194-208.  
13 Laureys, S., Boly, M., Maquet, P., 2006. Tracking the recovery of consciousness from coma.  
14 *J Clin Invest.* 116, 1823-5.  
15 Lisman, J.E., Jensen, O., 2013. The theta-gamma neural code. *Neuron.* 77, 1002-16.  
16 Lovsund, P., Oberg, P.A., Nilsson, S.E., 1980a. Magneto- and electrophosphenes: a  
17 comparative study. *Med Biol Eng Comput.* 18, 758-64.  
18 Lovsund, P., et al., 1980b. Magnetophosphenes: a quantitative analysis of thresholds. *Med  
19 Biol Eng Comput.* 18, 326-34.  
20 Mahjoory, K., et al., 2017. Consistency of EEG source localization and connectivity  
21 estimates. 152, 590-601.  
22 Modolo, J., et al., 2020. Decoding the circuitry of consciousness: from local microcircuits to  
23 brain-scale networks. *Network Neuroscience.* 4, 315-337.  
24 Rubinov, M., Sporns, O., 2010. Complex network measures of brain connectivity: uses and  
25 interpretations. *Neuroimage.* 52, 1059-69.  
26 Ruffini, G., 2017. An algorithmic information theory of consciousness. *Neurosci Conscious.*  
27 2017, nix019.  
28 Scheeringa, R., et al., 2016. The relationship between oscillatory EEG activity and the  
29 laminar-specific BOLD signal. *PNAS.* 113, 6761-66.  
30 Snyder, J.S., et al., 2012. Attention, awareness, and the perception of auditory scenes. *Front  
31 Psychol.* 3, 15.  
32 Tadel, F., et al., 2011. Brainstorm: a user-friendly application for MEG/EEG analysis.  
33 *Comput Intell Neurosci.* 2011, 879716.  
34 Thissen, D., Steinberg, L., Kuang, D., 2002. Quick and easy implementation of the  
35 Benjamini-Hochberg procedure for controlling the false positive rate in multiple comparisons.  
36 *Journal of Educational and Behavioral Statistics.* 27, 77-83.  
37 Tononi, G., 2004. An information integration theory of consciousness. *BMC Neurosci.* 5, 42.  
38 van Vugt, B., et al., 2018. The threshold for conscious report: Signal loss and response bias in  
39 visual and frontal cortex. *Science.* 360, 537-542.  
40 Watts, D.J., Strogatz, S.H., 1998. Collective dynamics of 'small-world' networks. *Nature.* 393,  
41 440-2.  
42 Xia, M., Wang, J., He, Y., 2013. BrainNet Viewer: a network visualization tool for human  
43 brain connectomics. *PLoS One.* 8, e68910.  
44  
45  
46  
47  
48  
49  
50  
51  
52  
53

**Acknowledgments: Funding:** This study is funded by Electricité de France (EDF, France),  
Réseau de Transport d'Electricité (RTE, France), Hydro-Québec (QC, Canada), and in part by  
the Future Emerging Technologies Open Luminous project (H2020-FETOPEN-2014-2015-

1  
2  
3 RIA under agreement No. 686764) as part of the European Union's Horizon 2020 research  
4 and training program 2014–2018. **Author contributions:** Conceptualization: JM, AL. Data  
5 curation: JM, AL. Formal analysis: JM, MH, AL. Funding acquisition: AL. Investigation: JM,  
6 AL. Methodology: JM, MH, GR, AL. Project administration: AL. Resources: AL. Software:  
7 JM, MH. Supervision: JM, AL. Validation: AL. Visualization: JM, MH, GR, AL. Writing  
8 (original draft): JM. Writing (review and editing): MH, GR, AL. **Data and materials**  
9 **availability:** EEG data and analysis pipeline details are available upon reasonable request.

10  
11  
12  
13  
14  
15  
16  
17  
18  
19  
20 "The authors have confirmed that any identifiable participants in this study have given their consent  
21 for publication".  
22  
23  
24  
25  
26  
27  
28  
29  
30  
31  
32  
33  
34  
35  
36  
37  
38  
39  
40  
41  
42  
43  
44  
45  
46  
47  
48  
49  
50  
51  
52  
53  
54  
55  
56  
57  
58  
59  
60